Graphical Synopsis

Inorganic Crystal Structures

Chang Xu, Shanrong Zhao, Jiaohua Zhou, Xu He and Haijun Xu

Crystallographic orientation of ilmenite inclusions in amphibole – an electron backscatter diffraction study

https://doi.org/10.1515/zkri-2020-0003
Z. Kristallogr. 2020; 235(4–5): 105–116

Synopsis: An EBSD technique is used to study the crystallographic relationships between ilmenite inclusions and amphibole host in a hornblendite. Four types of crystallographic relationships have been found, and their frequency is related to lattice coherency and oxygen packing.

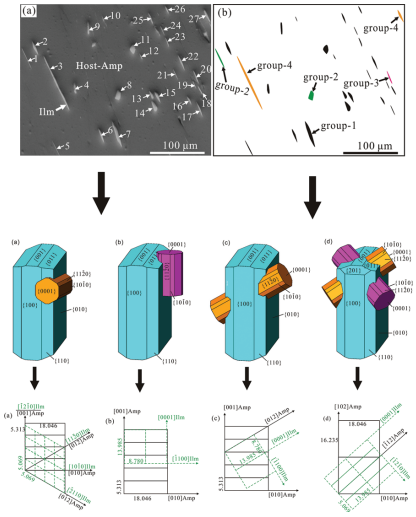

Myroslava Horiacha, Maximilian K. Reimann, Jutta Kösters, Vasyl' I. Zaremba and Rainer Pöttgen

Quaternary intermetallics $RE_2Pt_3Ga_4In$ (RE = Y, Gd-Tm) – intergrowth structures of $NdRh_2Sn_4$ and TiNiSi related slabs

https://doi.org/10.1515/zkri-2020-0012
Z. Kristallogr. 2020; 235(4–5): 117–125

Synopsis: Quaternary intermetallics $RE_2Pt_3Ga_4In$ (RE = Y, Gd-Tm) – Intergrowth structures of $NdRh_2Sn_4$ and TiNiSi related slabs.

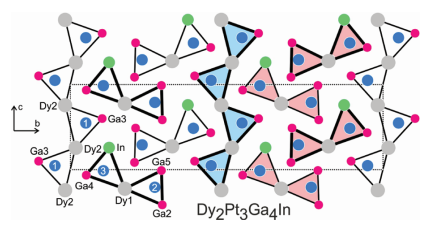

Olesya Timaeva, Vladimir Nikolaichik, Roman Svetogorov and Galina Kuz'micheva

Impact of the production method and diagnostics conditions on the compositions and structure of nanodimensional anatase

https://doi.org/10.1515/zkri-2019-0051
Z. Kristallogr. 2020; 235(4–5): 127–136

Synopsis: The two «core» – «shell» models with anatase nanoparticles and their associates as a core can be produced depending on the method.

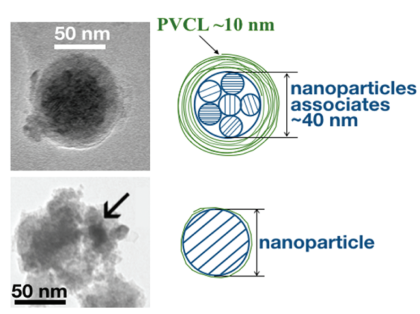

Maximilian K. Reimann and Rainer Pöttgen

Alkaline earth metal ordering in $CaCu_9Mg_2$ and $SrCu_9Mg_2$

https://doi.org/10.1515/zkri-2020-0031
Z. Kristallogr. 2020; 235(4–5): 137–141

Synopsis: $CaCu_9Mg_2$ and $SrCu_9Mg_2$ crystallize with a ternary ordered version of the $CeNi_3$ type with separate alkaline earth metal positions.

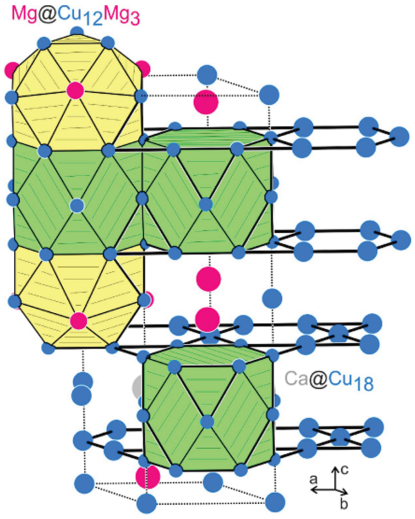

Michael Zoller, Rimma Bubnova, Yaroslav Biryukov, Eiken Haussühl, Rainer Pöttgen, Oliver Janka, Simon Penner, Corsin Praty, Harald Fitzek, Jörg Winkler, Stanislav Filatov and Hubert Huppertz

Elucidating the physical properties of the molybdenum oxide Mo_4O_{11} and its tantalum substituted variant $Mo_2Ta_2O_{11}$

https://doi.org/10.1515/zkri-2019-0073
Z. Kristallogr. 2020; 235(4–5): 143–155

Synopsis: Exploration of the properties of the three crystalline compounds γ/η-Mo_4O_{11} and $Mo_2Ta_2O_{11}$ with respect to their thermal and magnetic behavior, surface composition, and Raman spectroscopic properties.

Anton Shutov and Andrey Maleev

Coordination sequences of 2-uniform graphs

https://doi.org/10.1515/zkri-2020-0002
Z. Kristallogr. 2020; 235(4–5): 157–166

Synopsis: Explicit formulas for coordination sequences of all 20 plane 2-uniform graphs are proved. The method works for a wide class of plane periodic graphs.

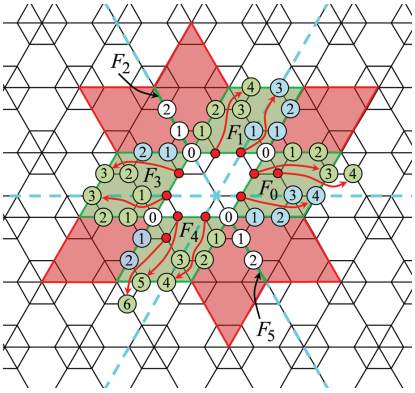

Anastasiia P. Topnikova, Elena L. Belokoneva, Olga V. Dimitrova, Anatoly S. Volkov and Leokadiya V. Zorina

Silicate-germanate $K_2Y[(Si_3Ge)O_{10}(OH)]$ with unusual complex corrugated layer and its correlation to ring silicate gerenite and chain silicate chkalovite

https://doi.org/10.1515/zkri-2020-0005
Z. Kristallogr. 2020; 235(4–5): 167–172

Synopsis: A new silicate-germanate $K_2Y[(Si_3Ge)O_{10}(OH)]$ synthesized hydrothermally has unusual corrugated layer consisting of (Si,Ge)-tetrahedra which are condensed by couples of YO_6-octahedra into the mixed microporous framework. K atoms are located in the channels (cross-section up to ~5.6 Å). This complex layer has similarity with ring silicate gerenite $(Ca,Na)_2(Y,REE)_3Si_6O_{18} \cdot 2H_2O$ and chain silicate chkalovite $Na_2BeSi_2O_6$.

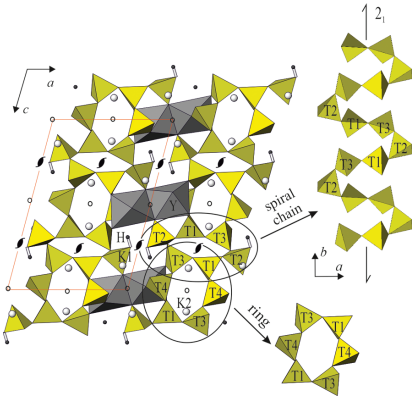

Letter

Formulae Index